E-ISSN: 3068-5052
Journal of Regenerative Medicine & Biology Research

ATHENAEUM SCIENTIFIC PUBLISHERS

Research Article

In-vitro Osteogenic Capacity and *In-vivo* Bone Healing of Porcine Freshly Isolated Adipose-Derived Stem Cells (ASC), CS34+ ASC and Bone Marrow-Derived Stem Cells

Massimo Bionaz[1,2], Tor W Jensen[2], Elisa Monaco[1], Aaron J Maki[1], RA Chanaka Rabel[1,2], Matthew B Wheeler[1,2*]

[1]Department of Animal Sciences, University of Illinois at Urbana-Champaign, Urbana, IL, 61801, USA

[2]Carl R Woese, Institute of Genomic Biology, University of Illinois at Urbana-Champaign, 1207 West Gregory Drive, Urbana, IL, 61801, USA

***Correspondence author:** Matthew B Wheeler, Ph.D., Professor of Developmental Biology, Department of Animal Sciences, Department of Bioengineering, Department of Biomedical and Translational Sciences Carle-Illinois College of Medicine, University of Illinois, 1207 West Gregory Drive Urbana, IL 61801; Email: mbwheele@illinois.edu

Citation: Bionaz M, et al. *In-vitro* Osteogenic Capacity and *In-vivo* Bone Healing of Porcine Freshly Isolated Adipose-Derived Stem Cells (ASC), CS34+ ASC and Bone Marrow-Derived Stem Cells. J Reg Med Biol Res. 2025;6(3):1-20.

https://doi.org/10.46889/JRMBR.2025.6306

Received Date: 02-12-2025

Accepted Date: 15-12-2025

Published Date: 23-12-2025

Abstract

Background: Both Adipose-Derived Stem Cells (ASCs) and Bone Marrow-Derived Stem Cells (BMSCs) have been successfully induced to undergo osteogenic differentiation *in-vitro* and *in-vivo*. Accordingly, we designed and conducted this study to test the osteogenic potential of Magnetic Cell Separation (MACS)-sorted ASCs compared to that of unsorted cells from SVF (unsorted ASCs; uASCs), Cultured-Sorted ASCs (CASCs) and unsorted cells from bone marrow aspirates (unsorted BMSCs; uBMSCs) for maxillofacial bone healing.

Methods: Using MACS, we sorted and isolated cells expressing the marker hematopoietic progenitor cell antigen sialomucin CD34 (CD34+; majority MSCs) and those not expressing the CD34 marker (CD34-) from freshly harvested SVF and compared *in-vitro* and i*n-vivo* osteogenic characteristics of MACS-derived ASCs (CD34+) to those of uASCs, CASCs and/ or uBMSCs. Based on our *in-vivo* experiments that involved heterologous transplantation of different cell types (uASCs, CD34+, CASCs and uBMSCs) into cylindrical surgical defects created on pig mandibles, bone healing capacities of uASCs and CD34+ were not different.

Findings: Among the different groups of ASCs used in the experiment, the highest *in-vivo* osteogenic potential was observed in CASCs. However, in our *in-vitro* and *in-vivo* experiments, the CD34+ group demonstrated a lower osteogenic capacity compared to uASCs.

Conclusion: Our findings indicate that cultured ASCs and uBMSCs have the highest osteogenic potential out of the different MSC populations we tested. Future studies should focus on identifying strategies for sorting MSCs with high-purity and minimal adverse effects to cellular physiology.

Keywords: Adipose-Derived Stem Cells; Porcine; Bone Regeneration; Craniofacial; Osteogenesis, Mandible; CD34

Abbreviations

ARS: Alizarin Red; ASCs: Adipose-Derive Stem Cells; API5: Apoptosis Inhibitor 5; BANF1: Barrier to Autointegration Nuclear Assembly Factor 1; BMA: Bone Marrow Aspirate; BMSCs: Bone Marrow-Derived Stem Cells; BTE: Bone Tissue Engineering; BSA: Bovine Serum Albumin; CFDA-SE: Carboxy-Fluorescein Diacetate Succinimidyl Ester; CASCs: Cultured-Sorted ASCs; CD34: Hematopoietic Progenitor Cell Antigen Sialomucin; CD34+: Cells Expressing the CD34 Marker; CD34-: Cells Not expressing the CD34 marker; COL1A1: Collagen Type I Alpha 1 Chain; CFU: Colony Forming Units; DEXA: Dual-Energy X-ray Absorptiometry; DMEM: Dulbecco' Modified Eagle's Medium; EPCs: Endothelial Progenitor Cells; FACS: Fluorescence-Activated Cell Sorting; GFP-ASCs: Green Fluorescent Protein Labelled ASCs; GAPDH: Glyceraldehyde-3-Phosphate Dehydrogenase; IACUC: Institutional Animal Care and Use Committee; iOR©: Intra-Operating Room; MACS: Magnetic Activated Cell Sorting; MACS-Sorted ASCs: CD34+ Cells that were Sorted but Not Cultured *in-vitro*; MSC: Mesenchymal Stem

Cells; MIX: Mixing CD34+ and CD34- Cells as per the CD34+: CD34- Ratio Determined by FACS; NSUN5= NOP2/Sun RNA Methyltransferase 5; PBS: Phosphate Buffered Saline; RPS15A: Ribosomal Protein S15a; SPARC: Secreted Protein Acidic and Rich in Cysteine (also known as Osteonectin); SVF: Stromal Vascular Fraction; uASCs: Unsorted ASCs; uBMSCs: Unsorted BMSCs

Introduction

Use of autologous bone grafts remains the gold standard for treatment/ repair of bone defects. However, given the challenges of using autologous bone (e.g. donor site morbidities, limitations in harvestable quantity), the osteogenic potential of Mesenchymal Stem Cells (MSCs) such as Adipose-Derived Stem Cells (ASCs) and Bone Marrow Stem Cells (BMSCs) has been thoroughly investigated over the last decade, both *in-vitro* and i*n-vivo*, in various animal species and humans [1-7]. However, even though ASCs and BMSCs have been successfully induced to undergo osteogenic differentiation Bone Tissue Engineering (BTE) both *in-vitro* and *in-vivo*, the extensive 'pre-clinical' research has not translated into 'clinical' patientcare yet. This is mainly due to two reasons. Firstly, MSC numbers in Bone Marrow Aspirates (BMAs) (BMAs) and Stromal Vascular Fractions (SVF) are typically low and insufficient to be transplanted back in the patient [8-10]. Secondly, BMAs and SVFs are heterogeneous mixes containing many types of cells in addition to the multi-potent MSCs [9,11,12].

In-vitro culture offers solutions to both above challenges; on the one hand, it will 'sort' MSCs up to near-100% purity within as few as two passages and on the other hand, it will cause massive *ex-vivo* expansion of the original MSC population [8,13]. However, *in-vitro* culture can take up to several weeks which makes the notion of one-step clinical applications [i.e. Intra-Operating Room (iOR©) MSC harvest and re-implantation within the same surgical procedure] impractical. Moreover, prolonged *in-vitro* culture of MSCs is known to increase incidence of genetic abnormalities and senescence and reduce proliferative capacity and stemness with every passage diminishing their usefulness in clinical applications [5,13-18]. Compared to ASCs, particularly BMSCs are reported to deteriorate in terms of morphological features, genetic stability, proliferative capacity and senescence during *in-vitro* culture [19-22]. In addition, some studies have shown a diminished ability of culture-derived MSCs to 'home in' on the site of tissue damage after systemic infusions [23].

On top of all of the above, from a regulatory perspective, the Food and Drug Administration (FDA) requires that MSCs be harvested, manipulated minimally and transplanted during the same surgical procedure in a one-step approach [24]. Boldly put, given the above-discussed biological and regulatory limitations, *in-vitro* culture cannot be used to sort and expand MSCs, if real-life BTE applications are to become realistic. Therefore, if clinical applications of MSCs in BTE are to become realistic, harvested MSCs must be used without multiplication, sorted or unsorted [24,25].

Even though many i*n-vivo* studies have been carried out using unsorted heterogeneous cell mixes from the SVF and BMA, the presence of different types of cells, especially those with intrinsic progenitor potential, poses risks of post-transplantation neoplasms and unwelcome tissue differentiation [24,26]. This is why non-culture methods of cell sorting such as Fluorescence-Activated Cell Sorting (FACS) are being extensively used in the field of BTE. Fluorescence-Activated Cell Sorting which uses cell-type specific markers to identify and sort different types of cells, is generally considered the gold standard for multi-parameter cell sorting. It has been used extensively to sort ASCs and BMSCs [27,28]. However, the relatively slow nature of the procedure and the relatively high cell loss incurred during the process (up to 70%) make FACS unsuitable for cell sorting procedures involving single-step autologous transplantations. Therefore, Magnetic Activated Cell Sorting (MACS), a sorting technology that is 4-6 times faster than FACS and with a lower rate of cell loss (<10%), has lately gained popularity in cell sorting applications involving BTE [28].

Considering this background information, we reasoned that ASCs have a better chance of being used in real-life BTE applications than BMSCs because the MSC count in SVFs can be up to 40 times greater than that in BMAs [12,29]. Therefore, ASC numbers in the SVF may be sufficient to be used in BTE applications directly, without the need for multiplication using *in-vitro* culture. In addition, as discussed elsewhere, ASCs have many other advantages over BMSCs in BTE applications [30]. We also reasoned that MACS is better suited than FACS for sorting ASCs considering the previously discussed benefits of MACS over FACS [28]. Taken together, we reasoned that MACS-sorted ASCs are most suitable for real-life BTE applications. Therefore, if ASCs can be harvested in sufficient quantities and efficiently sorted using MACS, they may be successfully used in autologous transplantations bypassing *in-vitro* culture and thereby satisfying FDA regulations (i.e. MSCs should be harvested and transplanted during the same surgical procedure, with minimal manipulations, in a one-step approach).

Based on the above reasoning, we designed and conducted this study to test the osteogenic potential of MACS-sorted ASCs compared to that of unsorted ASCs (uASCs), Cultivated ASCs (CASCs) and unsorted ASCs (uBMSCs). Adipose-derived stem cells are positive for the cell surface marker CD34 [31]. Therefore, CD34+ cells were sorted using MACS and used as MACS-sorted ASCs in this experiment. We compared the above cell populations using both *in-vitro* and i*n-vivo* experiments using porcine ASCs and a swine model. The relevance of the pig as a non-primate animal model for BTE applications has been reviewed elsewhere [32]. Our group had already demonstrated that transplantation of CASCs accelerates bone regeneration in surgical defects [7]. Therefore, in the current study, CASCs served not only as an internal control, but also to confirm and elaborate on prior findings [7].

For *in-vitro* experiments, we compared different cell populations for their capacity for forming CFU, osteogenic nodule formation and osteogenic marker gene expression. For i*n-vivo* experiments, cylindrical osteotomies were made on the mandibular rami of 20 pigs and the pigs were given intravenous injections containing one of the following six cell suspensions: (i) uASCs, (ii) CD34+ cells (MACS-sorted ASCs), (iii) CASCs, (iv) uBMSCs, (v) cultured-sorted GFP-ASCs or (vi) cell-free culture medium (as negative control). We added the cultured-sorted GFP-ASCs so we could determine if the infused cells participated in the healing of the defect.

The objective of this study was to test the osteogenic potential of MACS-sorted ASCs compared to that of unsorted cells from SVF (unsorted ASCs; uASCs), Culture-Sorted ASCs (CASCs) and unsorted cells from BMA (unsorted BMSCs; uBMSCs) for maxillofacial bone healing. We hypothesized that unsorted ASCs and BMSCs would have the highest osteogenic potential of all the cell treatments examined. Herewith, we present the results of the experiments conducted to compare the osteogenic potentials of uASCs, MACS-sorted ASCs, culture-sorted ASCs and uBMSCs.

Materials and Methods

Animals Used

For both *in-vitro* and *in-vivo* experiments, 6-12-month-old-pigs of the Yorkshire breed were used under protocols approved by the University of Illinois Institutional Animal Care and Use Committee (IACUC; Protocol #10014).

In-vitro Experiments

Harvest and Culture of ASCs

For the main *in-vitro* experiments, ASCs were isolated from the subcutaneous fat of the dorsal region (back fat) of four 6-month-old Yorkshire barrows (castrated males) immediately after euthanasia, as previously described [33]. In addition, using the same methods, ASCs were harvested from the back fat, peri-renal fat and mesenteric fat from two ~12-month-old-barrows to compare the osteogenic potential of ASCs from different fat depots.

All *in-vitro* experiments were performed using either 24-well plates (Cat# 3524, Corning, USA), 25 cm^2 flasks (Cat# 25100), 75 cm^2 flasks (Cat# 430641, Corning, USA) or 48-well plates (Cat# 353078, BD Falcon, USA). The protocols used for cell counting, cultivation, Colony-Forming Unit (CFU) assays and osteogenic differentiation were as described previously [33]. Where not specified, all centrifugations for obtaining cell pellets in the present and subsequent sections were performed at 200 × g.

Determination of CD34+ Cells by Flow Cytometry

Approximately one million freshly isolated cells from the SVF (i.e. uASCs) were fixed with 10% neutral-buffered formalin (Cat# 5725, Richard-Allan Scientific, USA) for at least 30 minutes, incubated with anti-CD34 primary mouse antibody (0.5μg /10^6 cells) for 45 minutes on ice and washed twice with Phosphate Buffered Saline (PBS) + 0.5% Bovine Serum Albumin (BSA) before incubating with R-phycoerythrin-conjugated secondary antibody (Goat anti-mouse IgG1; 1 μg/10^6 cells; Cat# P21129, Invitrogen, USA) for 30 minutes on ice. Stained cells were then rinsed twice with PBS + 0.5% BSA and incubated with anti-CD31 antibody for 30 minutes on ice (anti-pig FITC-conjugated CD31 antibody MCA1746F, AbD Serotec, USA). Finally, cells were rinsed twice and flow cytometer analysis (iCyt SY3200, Sony Biotechnology, Champaign, IL, USA) carried out at the Mills Breast Cancer Institute at Carle Hospital, Urbana, IL.

Enrichment for CD34+ by MACS

Unsorted ASCs were suspended in 200µL Dulbecco's Modified Eagle's Medium (DMEM; Cat# D5648, Sigma-Aldrich, USA) with 0.5% BSA (A8806, Sigma-Aldrich, USA), counted and treated with a homemade anti-porcine CD34 antibody preparation which were subsequently conjugated with Pierce™ Protein A/G Magnetic Beads (Cat# 88802, Thermo-Fisher, USA) following the manufacturer's protocols [34]. Then, CD34+ cells were sorted using MACS (Miltenyi Biotec, USA) and CD34+ and CD34- were counted using a hemocytometer. To account for the effect of sorting on the *in-vitro* experiment, a new group of cells was created by mixing CD34+ and CD34- cells (MIX) as per the CD34+: CD34- ratio determined by flow cytometry.

Colony-Forming Units Assay

The four groups of cells, i.e., uASCs, CD34+, CD34- and MIX were used for CFU in triplicate. The assay was done as described previously [33]. Briefly, cells were plated at a density of 1,000 cells/cm^2, cultured for nine days, fixed in formalin for 30 mins and the number of Colony-Forming Units (CFU) counted using an inverted microscope (Nikon Diaphot microscope). Clusters with ≥10 cells were counted as CFUs.

Osteogenic Nodule Characterization and Alizarin Red S Quantification

Unsorted ASCs, CD34+, CD34- and MIX were induced to differentiate toward the osteogenic lineage as described previously in 48-well plates [33]. Osteogenic nodules were observed using an inverted microscope at 100× magnification (Fig. 1). The number, radius and square area of osteogenic nodules were determined for each well and treatment using the image processing and analyzing software, Image J, according to the protocol described in Supplementary File 1. Briefly, a minimum of four photomicrographs were taken of each well and the radius and number of nodules were evaluated using bright-field photomicrographs on days 3, 6 and 18 of differentiation. Square area and mineralization of nodules were determined after fixing cells in 10% neutral-buffered formalin on day-18 of differentiation and treating them with Alizarin Red S (ARS), as previously described [35]. Briefly, mineralization was quantified by the extraction of the calcified mineral using acetic acid followed by neutralization with ammonium hydroxide. Colorimetric detection of the ARS solution was done at 520 nm absorbance using spectrophotometry (NanoDrop 1000, Thermo Scientific, USA). A 7-point standard curve with a 5-fold serial dilution using a known amount of ARS (2 g/L =5843.5µM) in a solution of acetic acid and ammonium hydroxide together with a negative control (solution of acetic acid and ammonium hydroxide without ARS) was used for precise quantification of µM ARS for each well.

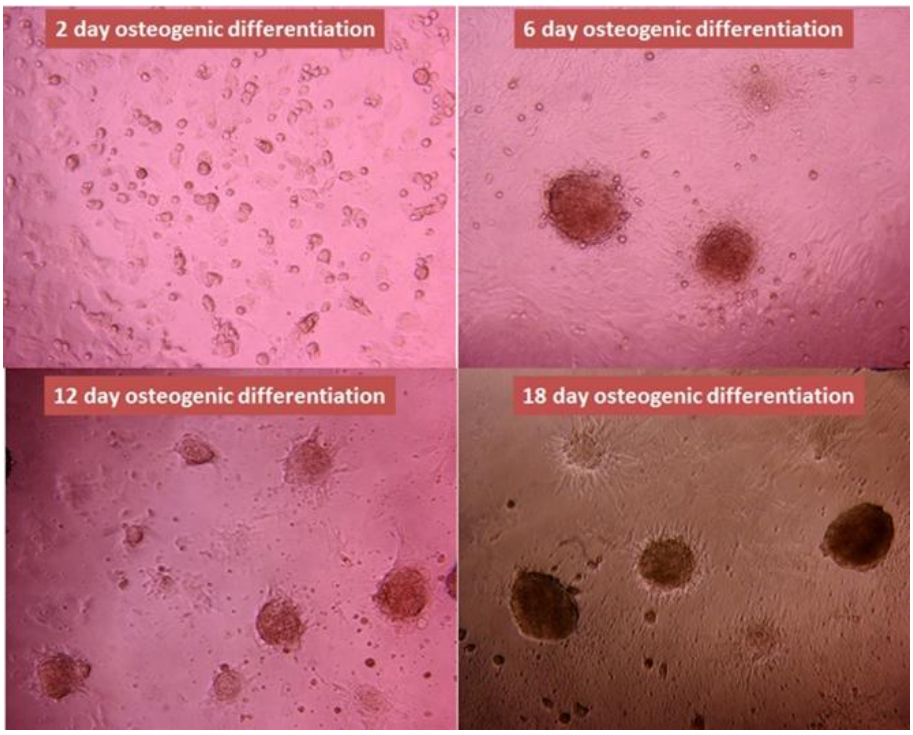

Figure 1: Bright-field photos at 100X of adipose stem cells at various days after osteogenic differentiation.

Real-Time Quantitative PCR (RT qPCR)

Nodules were harvested from uASCs, CD34+, CD34- and MIX groups on days 6, 12, 18, 26 and 34 after being induced to undergo osteogenic differentiation and RNA was extracted for RT-qPCR. Protocols for RNA isolation and RT-qPCR, including primer design, were performed as previously described [36]. The primer pairs for the osteogenic markers COL1A1 and SPARC and the internal control genes API5, NSUN5, RPS15A, BANF1 and GAPDH, were the same as previously reported [33,37]. The sequence of primer pair for CD34 was forward CTGCCTGCTGCTGGTCTTG and reverse GTTTTGGATGCTCATCTCTCTCAGT (exon-exon junction is underlined). The final RT-qPCR data were obtained by using a 6-point, 5-fold dilution standard curve. Analysis of the five internal control genes using geNorm revealed that the geometrical means of NSUN5, RPS15A and BANF1 provided the best normalization factor with a V-value of 0.159 [38].

In-vivo Experiments

Cell Isolation from Donor Pigs

The day before cell transplanting, subcutaneous fat (from the Stromal Vascular Fraction (SVF) and BMAs were obtained from back fat and femurs, respectively, from four Yorkshire donor pigs (2 females and 2 barrows aged 6-8 months and weighing 124±13 kg) as previously described [33]. Bone marrow aspirates from the two femurs (of a given animal) were mixed before further processing. Nucleated cells were stained with 4′,6-Diamidino-2-Phenylindole (DAPI) and counted using a fluorescence microscope (Olympus IX71, Center Valley, PA).

Enrichment for CD34+ by MACS

Part of the counted cells from the heterogeneous cell mix of the SVF was used for sorting CD34+ and CD34- using MACS, as described above in 'Enrichment for CD34+ by MACS' under the '*in-vitro* experiments' section of Materials and Methods. Sorted (CD34+ and CD34-) and unsorted cells (from SVF and BMA) were counted and incubated overnight in ultra-low attachment 75 cm^2 flasks (Cat# 3814, Corning, USA) at 39°C in 20 mL DMEM media with 10% FBS and antibiotics.

Mandible Defects and Cell Transplants

Twenty Yorkshire barrows (6.3±0.4 months of age) were used for the *in-vivo* study. Six bicortical cylindrical surgical defects of 10 mm diameter were created in the mandibular rami of each pig (three on each hemi-mandible; Fig. 2) following the surgical technique described previously [7]. Right hemi-mandible surgery was performed first in all cases. The most dorsal, ventral-rostral and the dorsal-caudal osteotomies were labeled as "up", "down" and "middle", respectively (Fig. 2). Post-surgical care was carried out as described previously [7].

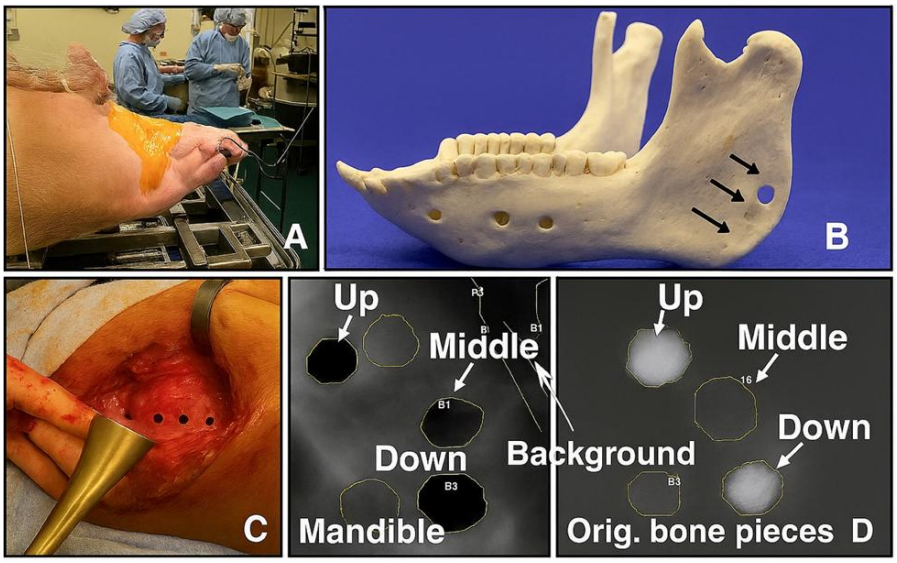

Figure 2: A) Surgical set up; B) Representation of a pig mandible with the three 10 mm round defects; C) The three 10 mm defects in the mandible just before closure of the surgical wound; D) Dual-Energy X-Ray Absorptiometry (DEXA) images of the

mandible with the 3 defects and the three pieces of bone removed from the defects and the background, all used to calculate the bone formation.

Even though the same type of trephine (10 mm outer diameter; Stryker, Portage, MI) was used to create the mandibular defects, the thickness of the lesion varied between pigs and even different regions of the same hemi-mandible (Fig. 3). Therefore, to accurately determine the quantity of bone that was removed and in turn, the quantity of bone that will be 'engineered' by ASCs *in-vivo*, bone extracted from the osteotomies were placed in Nasco Whirl-Pak bags, labeled with the osteotomy position (e.g. up, down, middle) and mandible side (e.g. left or right) and stored at -20^{0}C until analysis. The bone extracts were measured using Traceable® Digital Calipers (Fisher Scientific, USA) to ascertain the actual diameter and thickness of the respective defects. The measurements were also used as reference values when quantifying bone formation in osteotomies using DXA (Fig. 3).

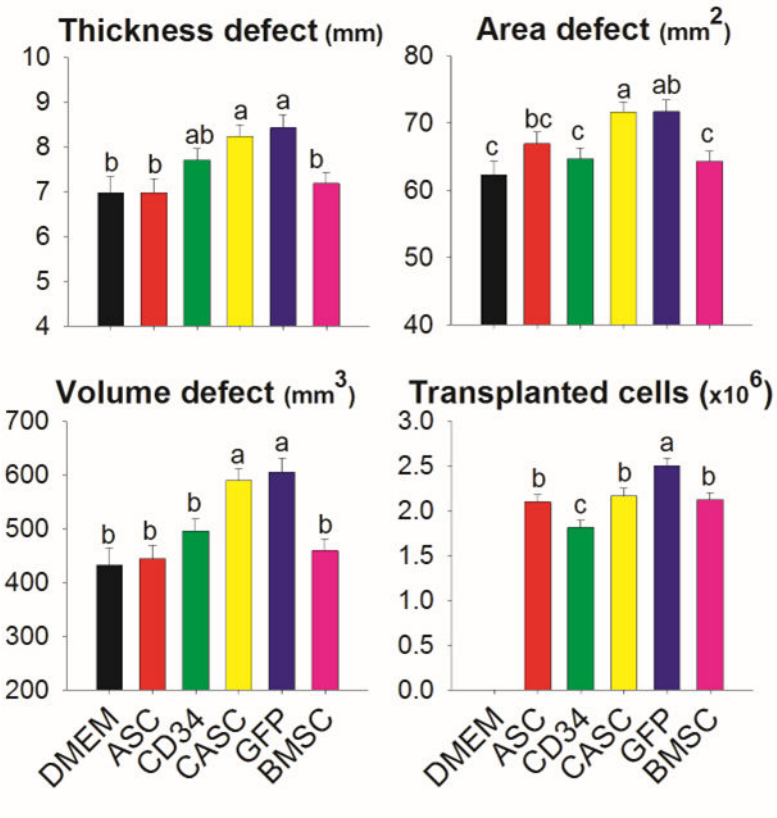

Figure 3: Thickness, area and volume of the defects and number of cells injected in ear vein for each of the treated pigs.

Upon completion of the surgeries, one of the following six treatments were administered intravenously through an ear vein catheter, as previously described [7]: (i) DMEM culture medium (i.e. negative control without cells; n=4 pigs), (ii) uASCs (n=3 pigs), (iii) CD34+ (CD34; n=3 pigs), (iv) uBMSCs (n=4 pigs), (v) passage-3 *in-vitro* cultured ASCs (CASCs; n=3 pigs) and (vi) passage-3 *in-vitro* cultured ASCs from a GFP transgenic pig (GFP; n=3 pigs). All IV infusions except the negative controls contained 2.14±0.41 ×10^6 cells of the relevant treatment suspended in 10 ml DMEM culture media. All cells, except GFP cells, were labelled with Carboxy-Fluorescein Diacetate Succinimidyl Ester (CFDA-SE) to allow post-harvest visualization of cells.

Carboxy-Fluorescein Diacetate Succinimidyl Ester (CFDA-SE) Labeling

Visualization of infused cells within the regenerated bone and/or surrounding soft tissues would help us to understand how they participate in tissue healing. Therefore, all cells except GFP expressing cells were labelled with a green fluorescence label, CFDA-SE (Cat# V12883, Invitrogen Grand Island, NY), before infusion into the pigs. A previously described protocol was followed with the exception of incubating cells at a higher dose of 30μM of CFDA-SE instead of 20μM, to further improve visualization of labeled cells in healed tissue [7]. All cells from a single donor were treated with CFDA-SE simultaneously so that they would be ready 30 minutes before the first transplant. Labeled cells were left in the dark at 37^{o}C until transplanting. Cells labeled with CFDA were transplanted 171±131 mins after preparation (30-372 mins). An aliquot of the cells from each donor, both treated and non-treated with CFDA-SE, was saved for counting and CFU assay.

Tissue Harvesting

Pigs were allowed to heal for four weeks, euthanized and the entire mandible extracted and fixed for at least one month prior to analysis, as described previously [7]. In addition, tissue samples from the area surrounding the surgical defect including skin, adipose tissue and muscle, were also fixed in 10% neutral buffered formalin to determine if transplanted cells have participated in soft tissue healing as well.

Dual-energy X-ray Absorptiometry Analysis (DXA)

Bone Mineral Density (BMD) of each defect was analyzed using a high-resolution method using a Hologic QDR 4500A system (45971, Hologic, Bedford, MA) and images were analyzed with Subregion Hi-Res 11.2.3 software (Hologic, Bedford, MA). The DXA analysis was similar to the previously described method except for using dimensions of the endogenous bone extracts to determine the volume and BMD of the newly synthesized bone [7]. The BMD was first calculated as BMD of the area of the defect minus the background (Fig. 2) and then corrected for the volume of the defect by multiplying by the thickness of the original defect to obtain BMD in grams of mineral/cm^3.

Analysis of Soft Tissue for the Presence of Fluorescent Cells

One of the objectives of the present study was to assess how transplanted cells participate in the healing of bone and surrounding soft tissue. This was evaluated by carefully dissecting the tissue surrounding the healing incision in both hemi-mandibles. We collected muscle tissue, adipose tissue and skin for this analysis. The tissue was fixed in 10% formalin for up to one month. The fixed soft tissue was cut into cubes (ca. 2 cm^3) and sectioned using a Leica CM3050 S cryostat at the Institute for Genomic Biology (University of Illinois at Urbana-Champaign). Sections of 10μm thickness were mounted on clean microscope slides and treated with xylene and toluidine blue solution before visualization using a stereomicroscope (Zeiss Stereolumar v12, Carl Zeiss, Germany) with a 1.5 lens (i.e., 150 x magnification). Photomicrographs were made using a GFP fluorescence filter and bright field microscopy using an Axiocam HRc high resolution color camera and the images were processed using the AxioVision software (Carl Zeiss, Germany). Slides with green fluorescence were further evaluated using a fluorescent (Olympus IX71 microscope, Center Valley, PA) microscope fitted with a monochromatic camera with a GFP filter to determine the presence of CFDA-labeled MSCs and GFP cells.

Statistical Analysis

All data were checked for outliers using Proc REG of SAS (v9.4) prior to statistical analysis. Data with a student's t-test value ≥3 were removed. Data were analyzed using Proc GLM of SAS, with main effects and various interactions (which were determined by the type of experiment) using pig or cell replicate as a random effect depending on the analysis. Effects and comparisons between treatments were considered statistically significant at $P \leq 0.05$. Statistical tendencies were accepted when $0.05 < P \leq 0.1$.

Results

To test how the osteogenic potential of CD34+ ASCs (MACS-sorted) compares to that of uASCs, culture-sorted ASCs and uBMSCs, we conducted several *in-vitro* and i*n-vivo* experiments using porcine ASCs and BMSCs. Briefly, *in-vitro* experiments were designed to test the osteogenic potential of ASCs from different fat depots of the body and sorted and unsorted groups of ASCs. Osteogenic nodule formation, colony-forming capacity and transcript dynamics of select genes were compared during *in-vitro* experiments. Our *in-vivo* experiments involved evaluating BMDs of *in-vivo* regenerated bone of pig mandibular surgical defects in response to intravenous infusion of sorted and unsorted ASCs and BMSCs. Herewith we present detailed findings of these *in-vitro* and *in-vivo* experiments.

Over 80% of CD34+ Cells are CD31- Cells

Of the cells in the SVF, CD34 is expressed not only by ASCs, but also by endothelial cells and Endothelial Progenitor Cells (EPCs). However, CD31 (PECAM-1) is expressed on endothelial cells and EPCs but not on ASCs. Flow cytometry of the SVFs revealed that >80% of CD34+ cells are CD34+/CD31- cells of a non-endothelial origin (Fig. 4) [39,40]. Therefore, the clear majority of MACS-sorted CD34+ cells can be considered as true MSCs. Those data are somewhat like prior data from another lab [31].

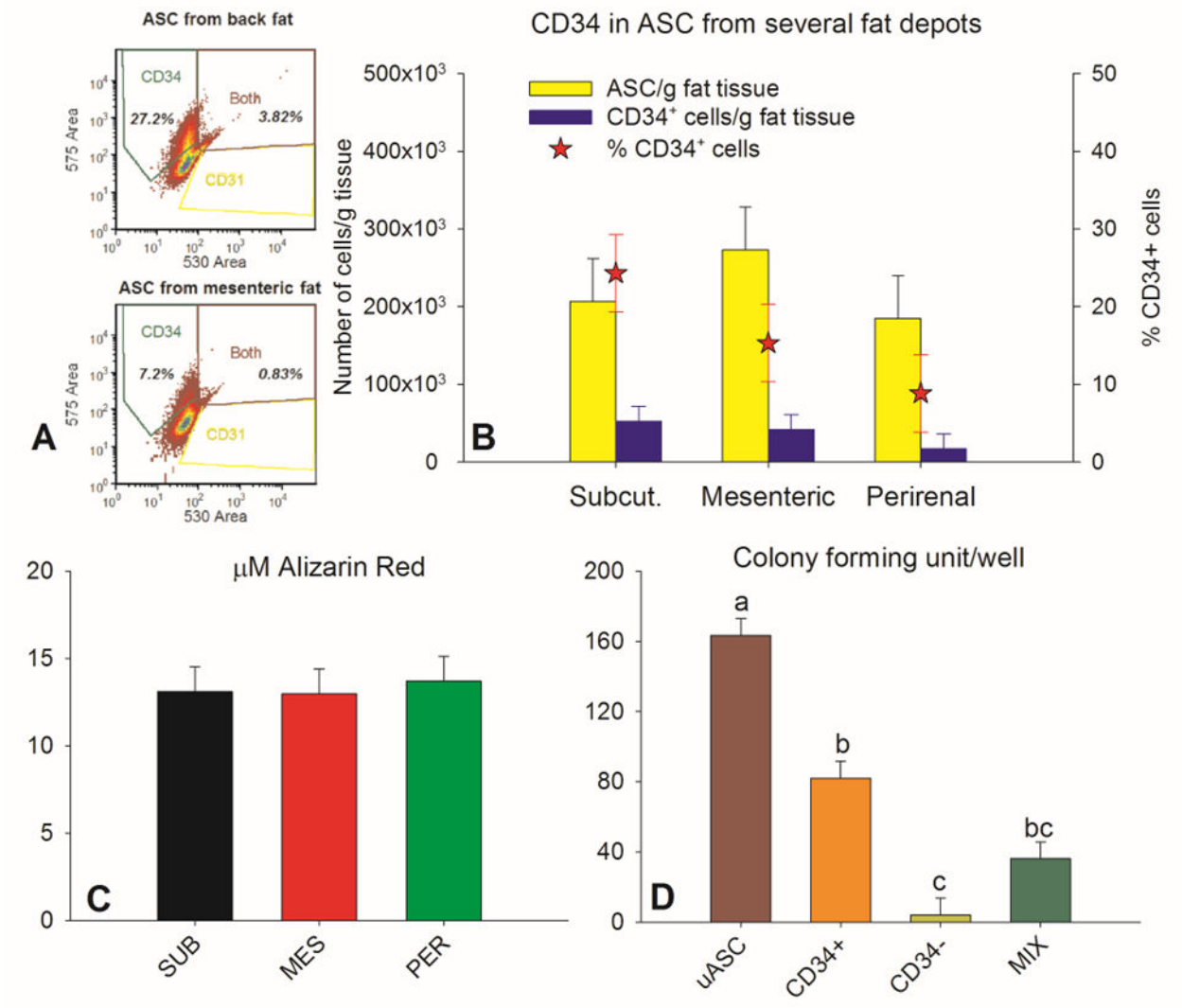

Figure 4: A: Flow cytometer analysis of ASC isolated from back subcutaneous and mesenteric adipose tissue depots. Representative Dot Plot displaying CD31-FITC on the x axis and CD34-PE on the y axis. CD31 is a specific endothelial marker. The control Dot Plot (upper left panel) denotes a sample with only secondary antibodies used to build the specific gates for CD34+, CD31+ and the gate denoting the combination of the two. The analysis highlighted an absence of CD31+/CD34- cells and a relative low proportion of CD34+/CD31+ cells and a relatively large proportion of CD34+ cells, particularly for the back subcutaneous and mesenteric adipose tissue; B: Number of cells/g tissue, number/ g tissue and % of CD34+ cells in ASC isolated from several adipose tissue depots in two 1-year old male pigs. The tissue effect was p=0.23 for % CD34+ cells, p=0.40 for number of CD34+ cells/g tissue and p=0.58 for number of cells/g tissue; C: Alizarin Red quantification of ASC isolated from Sub-cutaneous (SUB), Mesenteric (MES) and perirenal (PER) fat depot and cultivated in 48 well plate and differentiated for 19 days. D) Number of colonies with >10 cells in 48 well plate formed by unsorted ASC (uASC), CD34+ cells, CD34- cells and 50% mix of CD34+ and CD34- (MIX) after 6 days in culture isolated from a ca. 1 year old sow and sorted using MACS (every cell type was run in triplicates).

The Osteogenic Potential is Similar Among ASCs from Different Fat Depots

The number of cells, proportion of CD34+ and the osteogenic potential of cell isolates from back fat, peri-renal fat and mesenteric fat were compared. The number of harvested cells was highest in mesenteric fat and the proportion of CD34+ cells was highest in subcutaneous fat (Fig. 4). When induced to undergo osteogenic differentiation, the formation of osteogenic nodules, a typical feature of porcine ASCs undergoing osteogenic differentiation in a 2D environment was evident. Based on analyses of Alizarin Red S staining, the osteogenic potential of ASCs from the different fat depots was not different (Fig. 4) [33]. Therefore, from a clinical perspective, the usefulness of ASCs from subcutaneous fat would be as good as any other major internal fat deposit.

Colony-Forming Capacity of Unsorted and Sorted Cells is Different

Colony formation is a classical feature of mesenchymal cells. All four types of cells gave rise to colonies (Fig. 4). The highest number of CFU was observed in wells with unsorted cell cultures (P<0.05). Among the sorted cells, CD34+ gave rise to the highest number of colonies.

The Osteogenic Potential of Unsorted and Sorted Cells is Different

Before commencing culture, uASCs, CD34+, CD34- and MIX groups had similar CD34 transcript levels (Fig. 5). As reported by others in pigs as well as in humans, CD34 transcript levels steadily declined during the cell culture process [29,41,42]. In uASCs, the decline of CD34 transcript levels began after day 6 of culture. However, in other groups, the decline began before day 6 of culture. Further, CD34 transcript levels were consistently higher in the uASC group compared to other groups (P<0.05) (Fig. 5).

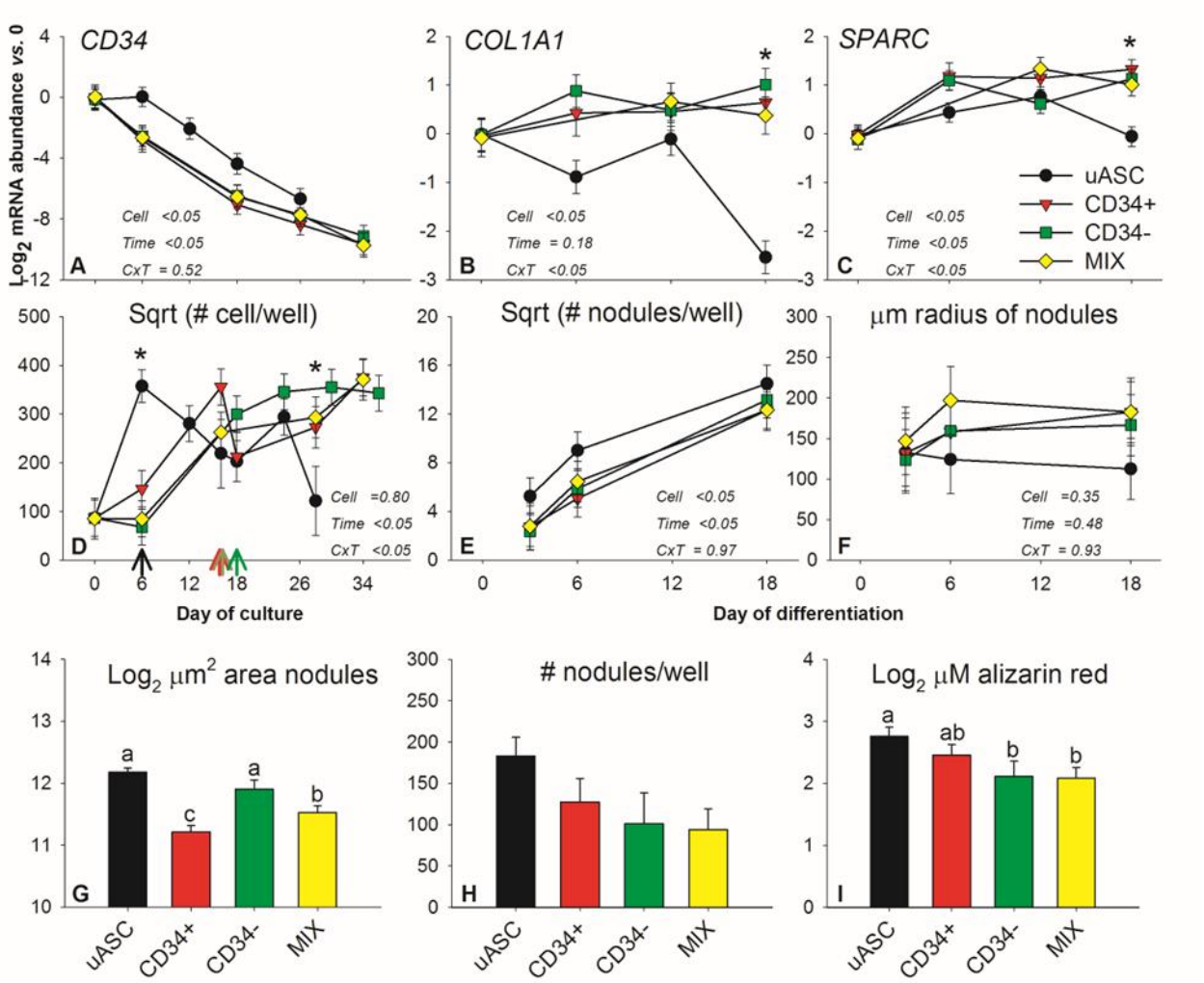

Figure 5: Transcription of CD34 (A) and osteogenic markers COL1A1 and SPARC (B and C), number of cells/well (D), number (E, H), radius (F), area (G) and content of alizarin red (I) of osteogenic nodules formed by unsorted ASC (uASC), cells sorted by using a CD34 antibody (CD34+), cells negative for CD34 (CD34-) and a mix of CD34+ and CD34- (MIX). Reported are the P-value of the effect of cell type (Cell), day of cultivation or day of osteogenic differentiation (Time) and their interaction (C×T). Data were log2- or square root (sqrt) - transformed before statistical analysis.

Over 18 days of *in-vitro* osteogenesis, transcript levels of COL1A1 decreased in uASCs while they increased in other groups (P<0.05; Fig. 5). During the same period, transcript levels of SPARC increased in all groups; however, a lesser increase was observed in uASCs than in other groups (P<0.05; Fig. 5). Transcript levels of both osteogenic markers is known to increase during the initial stage of *in-vitro* osteogenesis [33,43-45].

The pattern of SPARC expression in the present study is somewhat similar to our previous observation but COL1A1 is different, especially for uASC [33]. Those data are hard to reconcile and appear to indicate that COL1A1 might not be a consistent marker of osteogenesis in ASC. On the other side, the uASCs had a fast response to the osteogenic media with peak osteogenesis already at day 4 and thus, this might explain the lack of increase of those markers afterward. *In-vitro* osteogenic differentiation was induced when cells reached ~80% confluence in the wells. Unsorted ASCs, CD34+, MIX and CD34- groups reached ~80% confluence at ~ 6, ~16, ~16 and ~18 days after plating, respectively (Fig. 5). This observation, together with the number of CFU formed, suggests that MACS affects the normal physiology/proliferating capacity of cells in a detrimental manner. Osteogenic nodule formation was observed in all cell groups. The number of nodules increased consistently until the end of the trial (Fig. 5). Overall, uASCs gave rise to the highest number of nodules compared to other groups, particularly at the beginning of differentiation; however, the mean size of nodules was not different among different groups (Fig. 5).

Alizarin Red S staining at the end of the trial (i.e., 18 days of differentiation) revealed that nodules formed in CD34+ cells were smaller in size compared to the other groups ($P<0.05$; Fig. 5). The uASCs formed the highest number of nodules followed by CD34+ (Fig. 5). Calcium accumulation in the nodules of uASCs and CD34+ groups was significantly higher ($P<0.05$) than that in CD34- and MIX groups (Fig. 5).

In summary, of the four groups of cells tested, uASCs had the highest capacity for *in-vitro* proliferation and osteogenic differentiation suggesting that MACS affects the normal physiology/ stemness of cells in a detrimental manner. Interestingly, COL1A1 and SPARC transcript levels did not mirror the higher osteogenic capacity of uASCs. Contrary to our expectations, no differences were observed among CD34+, CD34- and MIX groups in terms of the number of nodules/well, mineralization or transcript levels of CD34, COL1A1 and SPARC. This relatively homogenous behavior of the three groups of sorted cells is likely a reflection of inefficient sorting by MACS resulting in relatively homogenous groups of cells. In other words, the retained fraction (CD34+ cells) has likely spilled over to the flow-through fraction (CD34- cells) during MACS, as reported by others [28]. The osteogenic potential of IV-transfused culture-sorted ASCs and BMSCs is greater than that of uASCs and CD34+. The average surface area of mandibular surgical defects was 67.1±8.0 mm^2/defect (total surface area of 403±47 mm^2/pig for all six defects). The average thickness of bicortical defects was 7.6±1.3 mm giving rise to an average volume of 510±124 mm^3/defect (3,059±589 mm^3/animal). Thus, a total bone volume of ~3 mL was removed with all six 10mm cylindrical defects per pig. In comparison, a single 25 mm osteotomy (critical size defect) removes a volume of 3.7 mL of native bone. Duration of mandibular surgeries was 1h, 49 min±39 mins. Pigs that received BMSCs and CASCs (both non-GFP and GFP cell lines) had the greatest levels of BMD among all the different treatments ($P<0.05$; Fig. 6). BMD levels observed in pigs that received CASC and BMSC were respectively 2.2 and 2-fold greater than pigs that received the negative control infusions. We had observed 3-fold differences in the past [7]. However, compared to the present study where ~$2x10^6$ CASCs were transfused intravenously per pig for six defects (<350,000 cells per defect), ~$5×10^6$ CASCs were transfused intravenously per pig for a single surgical defect during the aforementioned study. Therefore, despite transfusing ~14-fold fewer cells per defect compared to the previous study, CASCs significantly accelerated bone regeneration in the surgical defects [7].

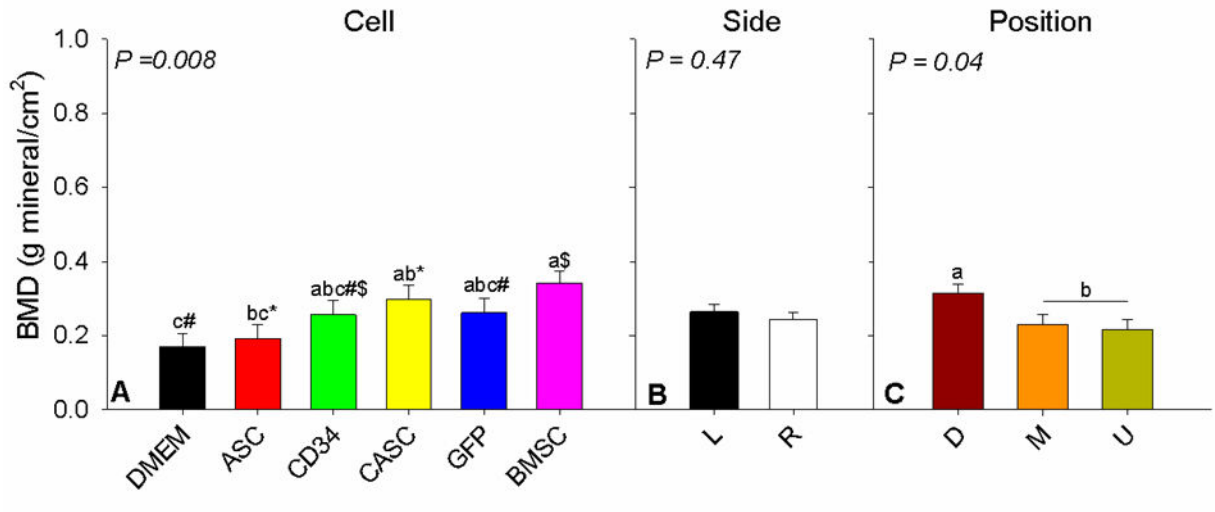

Figure 6: Bone Mineral Density (BMD) of bone defects in the mandible of pigs after 4 weeks of healing in conjunction with the intravenous injection of only media (DMEM), unsorted autologous Adipose Stem Cells (ASC), autologous CD34+ cells,

cultivated allogeneic Adipose Stem Cells (ASC), ASC obtained from Green-Fluorescent Transgenic Pigs (GFP) and autologous Bone Marrow Stem Cells (BMC). Shown are the effects of each cell type (Cell), side of the defect (left and right mandible), (Side) and position of the defect in the mandible: caudal (i.e., down or D), Medial (M) or cranial (i.e., upper or U) (Position). The statistical effect of the type of transplanted cells, side of the mandible and position of the defect are indicated. Different letters denote statistical effect between the various comparisons.

Bone mineral densities were not different between left and right hemi-mandibles of the same pig (Fig. 6). However, the most ventral defect (i.e., Down) showed a significantly greater level of bone healing compared to the other two locations ($P<0.05$; Fig. 6) despite presenting a larger volume defect due to the greater bone thickness of the location (Fig. 7). Thus, our data indicate that the ventral part of the mandible ramus (close to the body of the mandible) has a greater healing capacity compared to more dorsal regions of the ramus.

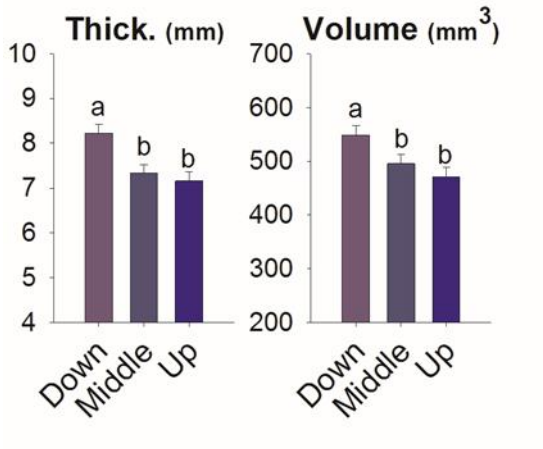

Figure 7: Thickness and volume of the 10 mm defects at the various various positions.

Unsorted ASCs and MACS-Sorted CD34+ Did Not Accelerate in-vivo Bone Regeneration

In contrast to CASCs and BMSCs, uASCs did not accelerate bone healing in the mandible defects ($P>0.05$; Fig. 6). Like our previous observations, levels of BMD observed in pigs that received uASCs were not different to that of the negative control (Fig. 6) [7]. Similar to uASCs, MACS-sorted CD34+ transplants did not accelerate bone healing in the pigs that received them (Fig. 6).

The critical size (i.e. a defect that does not allow spontaneous complete osseous regeneration during the animal's lifetime) for bicortical mandibular defects of pigs is 25 mm in diameter [46]. Therefore, it is likely that the defects that received the negative control transplants spontaneously healed by virtue of being <25 mm in diameter. Intravenous transfusions of uASCs or CD34+ did not accelerate spontaneous bone regeneration (Fig. 6). This is likely because only ~25% cells of the uASC infusion were true MSCs (Fig. 4) as opposed to near-100% MSCs in CASCs. In the case of CD34+, as observed with the *in-vitro* experiments, their cellular physiology/ stemness is likely modified/ compromised by MACS which likely attenuates their osteogenic potential and possibly even their ability to 'home-in' at the site of tissue injury.

In summary, with our *in-vivo* experiments, CASCs and BMSCs accelerated bone regeneration in non-critical sized surgical defects while uASCs and CD34+ did not. However, in most of our *in-vitro* experiments, uASCs outperformed CD34+.

Participation of CFDA-SE-Labeled Cells in Tissue Healing

Contrary to our prior observations, fluorescence microscopy could not confirm the presence of labeled cells within or around the surgical defects [7]. We also observed a decrease in CFU in cells treated with CFDA-SE (Fig. 8).

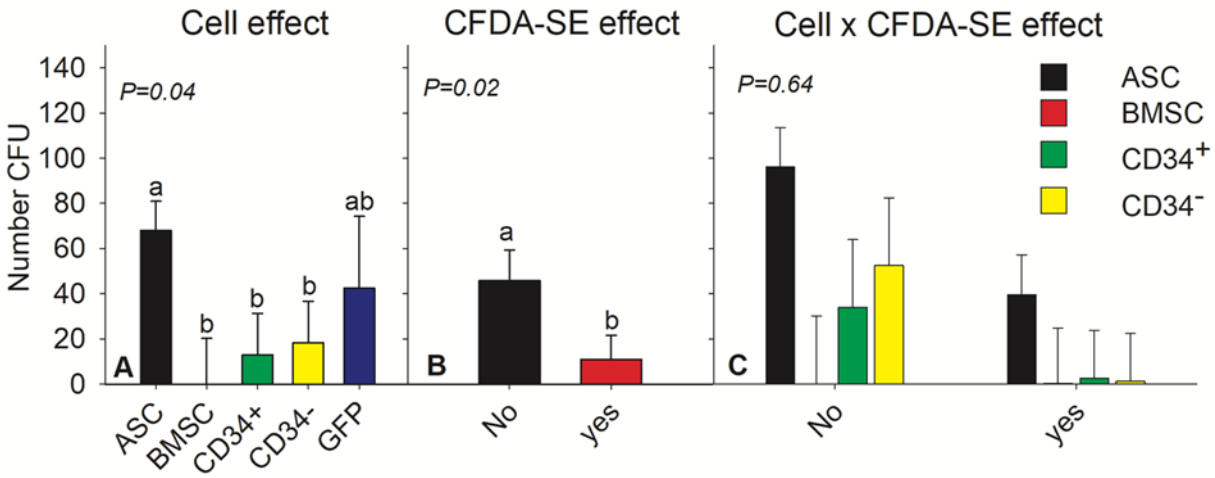

Figure 8: *In-vitro* number of colonies (in 25 cm² flask) of the same cells transplanted from the four donors. Effect of cell type with ASC being unsorted adipose stem cells, BMSC = bone marrow stem cells; cells isolated using antibodies against porcine CD34 (CD34+), cells left after the isolation with the CD34 antibodies (CD34-) and cells from a green fluorescent pig growth *in-vitro* (A): 30 µMol CFDA-SE treatment (B) Iinteraction of cell × CFDA-SE treatment were evaluated; (C): For the CFDA-SE effect and the interaction cell type × CFDA-SE the GFP cells were not considered. The number of colonies was overall affected by cell type ($P<0.05$) and the CFDA-SE treatment ($P=0.02$) but not by the interaction cell × CFDA-SE treatment ($P=0.64$).

Discussion

The extensive 'pre-clinical' research carried out over the last decade in engineering bone tissue from ASCs and BMSCs has not been translated into 'clinical' patientcare, to-date. One of the obstacles to this advancement has been the inability of current biotechnologies to satisfy certain regulations in effect. For example, certain FDA regulations (e.g., MSCs need to be harvested and transplanted during the same surgical procedure in a one-step approach, with minimal manipulations) preclude the use of *in-vitro* culture for multiplying and sorting MSCs. We reasoned that, compared to BMSCs, ASCs have a better chance of being successfully used in autologous BTE applications without the need for expansion (using *in-vitro* culture) because ASCs are available at a much higher concentration than BMSCs in freshly harvested aspirates. Magnetic Activated Cell Sorting is known to be faster and more efficient than Fluorescent Activated Cell Sorting (FACS) [28]. Therefore, we reasoned that MACS will be most suitable for sorting ASCs within a short period so that ASCs can be harvested, sorted and transplanted in a one-step approach satisfying the abovementioned FDA regulations. Therefore, the present study was designed to evaluate and compare the osteogenic potential of MACS-sorted ASCs to that of uASCs, culture-sorted ASCs and uBMSCs.

BMSCs vs ASCs: Not Just a Game of Numbers

Many previous studies that compared the osteogenic capacity of BMSCs and ASCs found that BMSCs had a stronger osteogenic potential than ASCs while others including our laboratory did not observe a difference in their osteogenic capacities [33,47-55]. Some of the above comparisons were only done *in-vitro* some did both *in-vitro* and *in-vivo* studies and a number of these studies were summarized in a review of the comparison between ASCs and BMSCs [47-50]. One study with human ASCs and BMSCs appears to have donor-matched cells but this is not specifically stated and whether they used more than one source of the cells is also not specified [47]. Another of these studies did donor-matched ASCs and BMSCs from three young donors (8-12 years of age) and tested the differentiation ability in nude rats [48]. They determined that ASCs were slower at growing bone in their *in-vivo* model [48]. A different group of investigators evaluated ASCs, BMSCs and Wharton's Jelly mesenchymal stem cells in both *in-vitro* and *in-vivo* models but the cell sources were not donor-matched [49]. The final study used non-donor matched ASCs (from donors 45-65 years of age) and BMSCs (from donors 52-73 years of age). These investigators found that BMSCs were superior in osteogenic and chondrogenic potential to the ASCs [50]. In a substantive review of several studies comparing ASCs and BMSCs in 2014 there was no clear cell source that was superior to the other as different studies showed both ASCs and BMSCs to be superior or inferior to the other cell source depending on the species used, assays performed and *in-vitro* or *in-vivo* model used [51]. In that context, the present study is unique in that ASCs and BMSCs were harvested from the same donors and

all donors were used for all of the treatments. Although we injected similar numbers of nucleated cells from each type (~2.1×10^6/pig), given that the BMSCs concentration in BMAs is much lower (<0.01% of nucleated total cells) than the ASCs concentration in SVFs, it should be emphasized that the number of actual BMSCs injected would have been considerably less than the number of actual ASCs injected [56]. Taken together, these observations suggest that even though BMSCs cannot be harvested in large numbers like ASCs, their potential for BTE clinical applications should not be underestimated based on numbers or rather, the lack of it.

uASCs Lack the Oomph?

One important observation from our study was that, in contrast to CASCs, uASCs did not accelerate *in-vivo* bone healing. The same was observed in another *in-vivo* study conducted using a rodent calvarial bone model where cultured ASCs showed greater proliferation, greater vascularization and greater bone volume regeneration compared to uASCs [57]. The same has been observed with BMSCs where cultured BMSCs showed greater *in-vivo* osteogenic potential compared to unsorted cells from freshly harvested BMAs in goats [58]. As stated earlier, the superior osteogenic potential of cultured ASCs and cultured BMSCs can be explained by the higher percentage of MSCs (near-100%) in them compared to the percentage of MSCs in SVF and BMA, respectively.

However, contradicting this explanation, many studies have reported the opposite, where uASCs had demonstrated greater osteogenic potential than cultured ASCs. Roato, et al., recognized the dilemma and explains the possible mechanisms behind it; "All those data open the debate on how it is possible that a smaller number of ASCs, present in freshly isolated SVF, compared to the expanded ASCs, could generate more tissue [30]. We believe that all the different cell populations present in SVF likely cooperate and stimulate mesenchymal cell activity better than the ASCs alone, confirming the fundamental interplay between stem cells and the microenvironment" [59].

Further, the inconsistency of outcomes among hundreds of BTE-related studies is well known and has been attributed to the differences of animal models, delivery methods, quantity and quality of cells used and various other intricacies of methodologies adopted by different investigators [30]. Therefore, more studies with consistent experimental designs and research methodologies are needed before concluding that cultured ASCs are superior to uASCs or vice versa. Regardless, it is important to remember that however strong the osteogenic potential of cultured MSCs may be, they cannot be used in BTE clinical applications, under the present circumstances. Therefore, it is vital that we, the scientific community, strategize and improvise to make unsorted MSCs work in the BTE arena.

MACS-Sorted CD34+ has Poor Osteogenic Potential?

One of the main objectives of the study was to test the osteogenic potential of MACS-sorted CD34+ so that the usefulness of MACS for sorting ASCs could be tested in an iOR® setting. Even though FACS is considered the gold standard for multi-parameter cell sorting, in comparison to MACS, FACS is known to be relatively slow (4-6 times slower than MACS), incur up to 70% cell-loss (vs <10% in MACS), impart high levels of shear stresses on cells, sort cells with a lower viability and to use more expensive equipment [28]. It was considering these deficiencies of FACS that we reasoned MACS was an overall better tool than FACS for sorting ASCs from the SVF in an iOR® setting.

Contrary to our predictions, MACS-sorted CD34+ demonstrated poor osteogenic potential in many of our *in-vitro* and *in-vivo* experiments. For example, among *in-vitro* studies, osteogenic nodule size was bigger with CD34- compared to CD34+ and no differences were observed between CD34- and CD34+ for the number, radius or ARS staining intensity of osteogenic nodules and mRNA levels of CD34, COL1A1 and SPARC. Among *in-vivo* studies, CD34+ group failed to accelerate bone regeneration. These 'poor performances' of CD34+ are likely due to one or more of the following reasons: (i) low efficiency of MACS in enriching CD34+ cells (ii) altered cellular physiology due to stresses exerted by MACS and (iii) purified and homogenous population of CD34+ is less potent than the synergistically cross-talking heterogeneous cell populations of uASC and uBMSC infusions [24,59-62]. However, the last of the above arguments can be refuted because our CASCs, which are essentially a culture-sorted, homogenous infusion of MSCs with near-100% purity, accelerated bone healing. Therefore, most likely, it is the poor efficiency of MACS and/or cellular stress exerted by MACS that resulted in the observed poor osteogenic potential of CD34+ cells.

The performance of the MIX group in our *in-vitro* experiments also supports the above notion that MACS affected cells in a negative manner. We created the MIX group by combining CD34+ and CD34- fractions in the CD34+: CD34- ratio obtained through FACS. Therefore, if MACS gave rise to pure CD34+ and CD34- fractions, the MIX would essentially have the same cellular composition as the SVF and hence should show the same osteogenic potential as uASCs. However, in all *in-vitro* comparisons, uASCs outperformed MIX, suggesting that the ratios were incorrect and/or cell function was compromised due to the stress exerted by MACS.

Our data suggests that the CD34- fraction from MACS would have been 'contaminated' with CD34+. Similarly, the CD34+ fraction may have been contaminated with CD34- cells. Others have also observed low purity rates of MACS-sorted fractions [63]. A recent publication reported that using manufacturer-recommended levels of antibodies and magnetic beads resulted in poor separation of the target cell type by MACS, especially when the target cell type and/or the surface molecule was present in large quantities [28]. In the SVF, ASCs, EPCs as well as endothelia express CD34 [64]. Even though our FACS detected only ~ 40% of the uASCs to be CD34+, others have reported that ASC and EPC can make up >80% of the cell population of the SVF [65-67]. Therefore, the CD34+ cell fraction in the SVF is very large and as such, the manufacturer-recommended antibody and magnetic bead concentrations may not have been sufficient to bind with all the CD34 surface molecules in our cell isolates. Consequently, MACS may have done only a partial job of sorting CD34+ in SVFs giving rise to relatively impure fractions of CD34+ and CD34-. We believe that this phenomenon played a considerable role in the current study resulting in 'poor performances' of CD34+. We suspect that the stress exerted by MACS also played a role in this 'poor performance' especially because our *in-vitro* studies showed that the proliferation rate of CD34+, CD34- and MIX groups was slower compared to that of uASCs.

For future studies of this nature, we strongly recommend the establishment of optimal concentrations of antibody and microbeads for optimal sorting of porcine SVF using MACS. The International Federation of Adipose Therapeutics and Science (IFATS) defines the surface marker profile of ASCs as positive/negative expression for four surface markers (CD34+/CD31−/CD45−/CD235a−), with an additional four markers (CD13, CD73, CD90 and CD105) for increased specificity [68]. However, following such strict guidelines results in very small numbers of enriched cells so the input to FACS/MACS needs to be extremely large to be able to output therapeutically useful numbers of ASC (~10^6-10^8). In contrast, using less restrictive surface marker profiles will allow isolation/sorting of larger cell populations with a relatively smaller starting number of cells [28]. Further, subjecting cells to multiple rounds of sorting with multiple sets of antibodies is not only expensive and time-consuming, but also stressful to cells and may compromise their cellular physiology/stemness. This is why we decided to sort SVF based on CD34 expression only. MACS-sorted CD34+ from SVF have been used in the regeneration of bone and other tissues successfully [69,70].

CFDA-SE Labeling Suppressed Cell Proliferation?

Donor cells transplanted were labeled with CFDA-SE before each surgery. However, not all cells were infused IV; aliquots of labeled and unlabeled cells were set aside to test their capacity for colony formation later point. It was observed that CFU counts for CFDA-SE-labeled cells were ~4 times lower ($P<0.05$) than those for unlabeled cells suggesting that CFDA-SE labeling suppressed cell proliferation *in-vitro*. As mentioned previously, GFP-ASCs were not treated with CFDA-SE. Therefore, GFP-ASC infused pigs would serve as an internal control to evaluate the *in-vivo* suppressive effects of CFDA-SE. However, it has been reported that GFP cells may be eliminated by non-GFP hosts due to presentation of GFP fragments by the major histocompatibility complex (MHC) [71]. If such an elimination took place in the present experiment as well, it would be incorrect to compare *in-vivo* data from CFDA-SE labelled cells and CFDA-SE non-labelled GFP cells.

If the abovementioned suppression observed *in-vitro* took place *in-vivo* as well, proliferation of ASCs and BMSCs and in turn osteogenic differentiation of MSCs and bone regeneration, would also have been compromised to a certain degree. Therefore, even though CASCs and uBMSCs accelerated *in-vivo* bone healing (~2-fold greater BMDs compared to negative controls), a greater level of acceleration would have taken place in the absence of the CFDA-SE-mediated suppression. This may be why only ~2-fold greater BMDs were observed in the current experiment (for CASCs compared to the negative control) compared to ~3-fold greater BMDs in our previous study [7].

We have used CFDA-SE labeling in our laboratory successfully without such mishaps in the past [7]. In those studies, porcine ASCs have shown good fluorescence up to four weeks post-transplantation when labeled using a 20 μM solution. However, in the current study, we used a 30 μM solution to label cells with the hope of visualizing stronger fluorescence. Contrary to our

expectation, the higher concentration appears to have been inhibitory to cellular functions. The optimum concentration of CFDA-SE depends on the cell type being labeled and excessively high concentrations and prolonged incubation periods are known to be cytotoxic and impair the ability of cells to divide [72]. Lack of green fluorescence within or around the healed surgical defects in this study may be an effect of the cytotoxicity of high concentrations of CFDA-SE. Generally, the green fluorescence is known to be detectable up to eight cell divisions at which point the fluorescence decreases to background levels [73].

CFDA-SE concentrations as low as 0.5μM have proven to be effective in other cell types [74]. Future studies to determine the optimum concentration for porcine ASCs are warranted to avoid mishaps of this nature.

Successful IV Transplantation of MSCs

Concerns have been raised about IV-infused MSCs getting trapped in the lungs and not reaching the target site [75]. However, our group has disproved this claim in our previous studies [7,76]. Thus we expect this not to be an issue in the present study.

Summary and Conclusions

Several important findings came out of this study. Culture-sorted ASCs and unsorted BMSCs from BMAs accelerated *in-vivo* bone healing. Based on BMDs of newly synthesized bone, CASCs and uBMSCs showed similar *in-vivo* bone healing potential. This observation is of great interest because the actual number of MSCs in the uBMSCs infusion would have been many thousands of times less than the number of MSCs in the CASC infusion. This observation challenges the current position of several studies that consider ASCs to be more valuable than BMSCs in BTE applications. Even though BMSCs have many limitations (related to harvesting of the BMA and MSC concentration in the BMA) compared to ASCs, our findings indicate the need for further research in this area. Contrary to our predictions, MACS-sorted CD34+ did not accelerate *in-vivo* bone healing. Findings from *in-vitro* experiments suggest that MACS may have altered cellular physiology and that sorting may have been partial. Poor osteogenic potential shown by CD34+ is likely due to these reasons. *In-vitro*, unsorted cells from SVFs (uASCs) showed superior osteogenic nodule formation, CFU and osteogenic gene expression dynamics compared to MACS-sorted cells. However, *in-vivo*, like CD34+, uASCs did not accelerate bone healing. In contrast to a previous study from our laboratory, the fold-change difference of BMDs observed in *in-vivo* synthesized bone (in comparison to the negative controls), was lower in the current study. This may be due to the smaller number of cells infused IV (~350,000 per defect) in comparison to the previous study (5 million per defect) and/or a possible CFDA-SE labeling-mediated inhibition on the proliferation of transplanted cells.

Conflict of Interest

The authors declare no conflicts of interest.

Funding Statement

This work was supported by a grant from the Illinois Regenerative Medicine Institute IDPH 63080017 through the State of Illinois Department of Public Health.

Availability of Data and Materials

The entirety of the data described is included in the published article and supplemental materials.

Acknowledgements

The authors thank the staff, especially Mr. Jonathan Mosely, the Unit Manager, at the Imported Swine Research Laboratory, for their diligent and uncompromising care of the animals.

References

1. Monaco E, Bionaz M, Hollister SJ, Wheeler MB. Strategies for regeneration of the bone using porcine adult adipose-derived mesenchymal stem cells. Theriogenology. 2011;75(8):1381-99.
2. Levi B, Longaker MT. Concise review: Adipose-derived stromal cells for skeletal regenerative medicine. Stem cells. 2011;29(4):576-82.
3. Tsuji W, Rubin JP, Marra KG. Adipose-derived stem cells: Implications in tissue regeneration. World J Stem Cells. 2014;6(3):312-21.
4. Gaubys A, Papeckys V, Pranskunas M. Use of autologous stem cells for the regeneration of periodontal defects in animal

studies: A systematic review and meta-analysis. J Oral Maxillofac Res. 2018;9(2):e3.
5. Mende W, Götzl R, Kubo Y, Pufe T, Ruhl T, Beier JP. The role of adipose stem cells in bone regeneration and bone tissue engineering. Cells. 2021;10(5).
6. Rahman G, Frazier TP, Gimble JM, Mohiuddin OA. The emerging use of ASC/Scaffold composites for the regeneration of osteochondral defects. Front Bioeng Biotechnol. 2022;10:893992.
7. Wilson SM, Goldwasser MS, Clark SG, Monaco E, Bionaz M, Hurley WL, et al. Adipose-derived mesenchymal stem cells enhance healing of mandibular defects in the ramus of swine. Journal of oral and maxillofacial surgery: Official journal of the American Association of Oral and Maxillofacial Surgeons. 2012;70(3):e193-203.
8. Pittenger MF, Mackay AM, Beck SC, Jaiswal RK, Douglas R, Mosca JD, et al. Multilineage potential of adult human mesenchymal stem cells. Science. 1999;284(5411):143-7.
9. Song JH, Kim J-W, Lee MN, Oh S-H, Piao X, Wang Z, et al. Isolation of high purity mouse mesenchymal stem cells through depleting macrophages using liposomal clodronate. Tissue Engineering and Regenerative Medicine. 2022;19(3):565-75.
10. Astori G, Vignati F, Bardelli S, Tubio M, Gola M, Albertini V, et al. "*In-vitro*" and multicolor phenotypic characterization of cell subpopulations identified in fresh human adipose tissue stromal vascular fraction and in the derived mesenchymal stem cells. J Transl Med. 2007;5:55.
11. Chahla J, Mannava S, Cinque ME, Geeslin AG, Codina D, LaPrade RF. bone marrow aspirate concentrate harvesting and processing technique. Arthrosc Tech. 2017;6(2):e441-e5.
12. Han S, Sun HM, Hwang KC, Kim SW. Adipose-derived stromal vascular fraction cells: Update on clinical utility and efficacy. Crit Rev Eukaryot Gene Expr. 2015;25(2):145-52.
13. Brooks AES, Iminitoff M, Williams E, Damani T, Jackson-Patel V, Fan V, et al. *Ex-vivo* Human adipose tissue derived mesenchymal stromal cells (ASC) are a heterogeneous population that demonstrate rapid culture-induced changes. Front Pharmacol. 2019;10:1695.
14. Lo Surdo JL, Millis BA, Bauer SR. Automated microscopy as a quantitative method to measure differences in adipogenic differentiation in preparations of human mesenchymal stromal cells. Cytotherapy. 2013;15(12):1527-40.
15. Wall ME, Bernacki SH, Loboa EG. Effects of serial passaging on the adipogenic and osteogenic differentiation potential of adipose-derived human mesenchymal stem cells. Tissue Eng. 2007;13(6):1291-8.
16. Mitchell JB, McIntosh K, Zvonic S, Garrett S, Floyd ZE, Kloster A, et al. Immunophenotype of human adipose-derived cells: Temporal changes in stromal-associated and stem cell-associated markers. Stem Cells. 2006;24(2):376-85.
17. Legzdina D, Romanauska A, Nikulshin S, Kozlovska T, Berzins U. Characterization of Senescence of Culture-expanded Human Adipose-derived Mesenchymal Stem Cells. Int J Stem Cells. 2016;9(1):124-36.
18. Neri S, Bourin P, Peyrafitte JA, Cattini L, Facchini A, Mariani E. Human Adipose Stromal Cells (ASC) for the regeneration of injured cartilage display genetic stability after *in-vitro* culture expansion. PLoS One. 2013;8(10):e77895.
19. Baxter MA, Wynn RF, Jowitt SN, Wraith JE, Fairbairn LJ, Bellantuono I. Study of telomere length reveals rapid aging of human marrow stromal cells following *in-vitro* expansion. Stem Cells. 2004;22(5):675-82.
20. Choudhery MS, Badowski M, Muise A, Pierce J, Harris DT. Donor age negatively impacts adipose tissue-derived mesenchymal stem cell expansion and differentiation. J Transl Med. 2014;12:8.
21. Stolzing A, Jones E, McGonagle D, Scutt A. Age-related changes in human bone marrow-derived mesenchymal stem cells: consequences for cell therapies. Mech Ageing Dev. 2008;129(3):163-73.
22. Zaim M, Karaman S, Cetin G, Isik S. Donor age and long-term culture affect differentiation and proliferation of human bone marrow mesenchymal stem cells. Ann Hematol. 2012;91(8):1175-86.
23. Rombouts WJ, Ploemacher RE. Primary murine MSC show highly efficient homing to the bone marrow but lose homing ability following culture. Leukemia. 2003;17(1):160-70.
24. Dykstra JA, Facile T, Patrick RJ, Francis KR, Milanovich S, Weimer JM, et al. Concise review: Fat and furious: harnessing the full potential of adipose-derived stromal vascular fraction. Stem Cells Transl Med. 2017;6(4):1096-108.
25. Guo J, Nguyen A, Banyard DA, Fadavi D, Toranto JD, Wirth GA, et al. Stromal vascular fraction: A regenerative reality? Part 2: Mechanisms of regenerative action. Journal of Plastic, Reconstructive and Aesthetic Surgery. 2016;69(2):180-8.
26. Prockop DJ, Olson SD. Clinical trials with adult stem/progenitor cells for tissue repair: Let's not overlook some essential precautions. Blood. 2007;109(8):3147-51.
27. Dadras M, May C, Wagner JM, Wallner C, Becerikli M, Dittfeld S, et al. Comparative proteomic analysis of osteogenic differentiated human adipose tissue and bone marrow-derived stromal cells. J Cell Mol Med. 2020;24(20):11814-27.

28. Sutermaster BA, Darling EM. Considerations for high-yield, high-throughput cell enrichment: Fluorescence versus magnetic sorting. Scientific Reports. 2019;9(1):227.
29. Varma MJ, Breuls RG, Schouten TE, Jurgens WJ, Bontkes HJ, Schuurhuis GJ, et al. Phenotypical and functional characterization of freshly isolated adipose tissue-derived stem cells. Stem cells and development. 2007;16(1):91-104.
30. Le Q, Madhu V, Hart JM, Farber CR, Zunder ER, Dighe AS, et al. Current evidence on potential of adipose derived stem cells to enhance bone regeneration and future projection. World J Stem Cells. 2021;13(9):1248-77.
31. Liu YJ, Zhang TY, Tan PC, Zhang PQ, Xie Y, Li QF, et al. Superiority of Adipose-derived CD34 + cells over adipose-derived stem cells in promoting ischemic tissue survival. Stem Cell Rev Rep. 2022;18(2):660-71.
32. Rubessa M, Polkoff K, Bionaz M, Monaco E, Milner DJ, Holllister SJ, et al. Use of pig as a model for mesenchymal stem cell therapies for bone regeneration. Anim Biotechnol. 2017;28(4):275-87.
33. Monaco E, Sobreira de Lima A, Bionaz M, Maki A, Wilson MS, Hurley WL, et al. Morphological and transcriptomic comparison of adipose and bone marrow derived porcine stem cells. The Open Tissue Engineering and Regenerative Medicine Journal. 2009;2:20-33.
34. Jensen TW, Swanson DA, Rund LA, Kim K, Clark-Deener SG, Schook LB, editors. A Type I monoclonal antibody identifies a common epitope on multiple isoforms of the porcine CD34 antigen. Swine in Biomedical Research Conference. 2011;2011.
35. Gregory CA, Gunn WG, Peister A, Prockop DJ. An Alizarin red-based assay of mineralization by adherent cells in culture: Comparison with cetylpyridinium chloride extraction. Anal Biochem. 2004;329(1):77-84.
36. Bionaz M, Loor JJ. Identification of reference genes for quantitative real-time PCR in the bovine mammary gland during the lactation cycle. Physiological Genomics. 2007;29(3):312-9.
37. Monaco E, Bionaz M, Sobreira de Lima A, Hurley WL, Loor JJ, Wheeler MB. Selection and reliability of internal reference genes for quantitative PCR verification of transcriptomics during the differentiation process of porcine adult mesenchymal stem cells. Stem Cell Research and Therapy. 2010;1(1):7.
38. Vandesompele J, De Preter K, Pattyn F, Poppe B, Van Roy N, De Paepe A, et al. Accurate normalization of real-time quantitative RT-PCR data by geometric averaging of multiple internal control genes. Genome Biology. 2002;3(7).
39. Muller AM, Hermanns MI, Skrzynski C, Nesslinger M, Muller KM, Kirkpatrick CJ. Expression of the endothelial markers PECAM-1, vWf and CD34 *in-vivo* and *in-vitro*. Experimental and molecular pathology. 2002;72(3):221-9.
40. Tárnok A, Ulrich H, Bocsi J. Phenotypes of stem cells from diverse origin. Cytometry A. 2010;77(1):6-10.
41. Williams KJ, Picou AA, Kish SL, Giraldo AM, Godke RA, Bondioli KR. Isolation and characterization of porcine adipose tissue-derived adult stem cells. Cells Tissues Organs. 2008;188(3):251-8.
42. Feisst V, Brooks AE, Chen CJ, Dunbar PR. Characterization of mesenchymal progenitor cell populations directly derived from human dermis. Stem Cells Dev. 2014;23(6):631-42.
43. Köllmer M, Buhrman JS, Zhang Y, Gemeinhart RA. Markers are shared between adipogenic and osteogenic differentiated mesenchymal stem cells. J Dev Biol Tissue Eng. 2013;5(2):18-25.
44. Luo Y, Ge R, Wu H, Ding X, Song H, Ji H, et al. The osteogenic differentiation of human adipose-derived stem cells is regulated through the let-7i-3p/LEF1/β-catenin axis under cyclic strain. Stem Cell Res Ther. 2019;10(1):339.
45. Padial-Molina M, de Buitrago JG, Sainz-Urruela R, Abril-Garcia D anderson P, O'Valle F, et al. Expression of Musashi-1 during osteogenic differentiation of oral MSC: An *in-vitro* Study. Int J Mol Sci. 2019;20(9).
46. Dewey MJ, Milner DJ, Weisgerber D, Flanagan CL, Rubessa M, Lotti S, et al. Repair of critical-size porcine craniofacial bone defects using a collagen-polycaprolactone composite biomaterial. bioRxiv. 2021:2021.04.19.440506.
47. Xu L, Liu Y, Sun Y, Wang B, Xiong Y, Lin W, et al. Tissue source determines the differentiation potentials of mesenchymal stem cells: A comparative study of human mesenchymal stem cells from bone marrow and adipose tissue. Stem Cell Res Ther. 2017;8(1):275.
48. Mohamed-Ahmed S, Yassin MA, Rashad A, Espedal H, Idris SB, Finne-Wistrand A, et al. Comparison of bone regenerative capacity of donor-matched human adipose-derived and bone marrow mesenchymal stem cells. Cell Tissue Res. 2021;383(3):1061-75.
49. Kargozar S, Mozafari M, Hashemian SJ, Brouki Milan P, Hamzehlou S, Soleimani M, et al. Osteogenic potential of stem cells-seeded bioactive nanocomposite scaffolds: A comparative study between human mesenchymal stem cells derived from bone, umbilical cord Wharton's jelly and adipose tissue. J Biomed Mater Res B Appl Biomater. 2018;106(1):61-72.
50. Im GI, Shin YW, Lee KB. Do adipose tissue-derived mesenchymal stem cells have the same osteogenic and chondrogenic potential as bone marrow-derived cells? Osteoarthritis Cartilage. 2005;13(10):845-53.

51. Liao HT, Chen CT. Osteogenic potential: Comparison between bone marrow and adipose-derived mesenchymal stem cells. World J Stem Cells. 2014;6(3):288-95.
52. Stockmann P, Park J, von Wilmowsky C, Nkenke E, Felszeghy E, Dehner JF, et al. Guided bone regeneration in pig calvarial bone defects using autologous mesenchymal stem/progenitor cells - a comparison of different tissue sources. J Craniomaxillofac Surg. 2012;40(4):310-20.
53. Kang BJ, Ryu HH, Park SS, Koyama Y, Kikuchi M, Woo HM, et al. Comparing the osteogenic potential of canine mesenchymal stem cells derived from adipose tissues, bone marrow, umbilical cord blood and Wharton's jelly for treating bone defects. J Vet Sci. 2012;13(3):299-310.
54. Kern S, Eichler H, Stoeve J, Kluter H, Bieback K. Comparative analysis of mesenchymal stem cells from bone marrow, umbilical cord blood or adipose tissue. Stem Cells. 2006;24(5):1294-301.
55. Monaco E, Bionaz M, Rodriguez-Zas S, Hurley WL, Wheeler MB. Transcriptomics comparison between porcine adipose and bone marrow mesenchymal stem cells during *in-vitro* osteogenic and adipogenic differentiation. PloS One. 2012;7(3):e32481.
56. Cotter EJ, Wang KC, Yanke AB, Chubinskaya S. Bone Marrow Aspirate Concentrate for Cartilage Defects of the Knee: From Bench to Bedside Evidence. Cartilage. 2018;9(2):161-70.
57. Cheung WK, Working DM, Galuppo LD, Leach JK. Osteogenic comparison of expanded and uncultured adipose stromal cells. Cytotherapy. 2010;12(4):554-62.
58. Kruyt MC, de Bruijn JD, Yuan H, van Blitterswijk CA, Verbout AJ, Oner FC, et al. Optimization of bone tissue engineering in goats: A peroperative seeding method using cryopreserved cells and localized bone formation in calcium phosphate scaffolds1. Transplantation. 2004;77(3):359-65.
59. Roato I, Belisario DC, Compagno M, Verderio L, Sighinolfi A, Mussano F, et al. Adipose-derived stromal vascular fraction/xenohybrid bone scaffold: An alternative source for bone regeneration. Stem Cells International. 2018;2018:4126379.
60. Xu C, Liu H, He Y, Li Y, He X. Endothelial progenitor cells promote osteogenic differentiation in co-cultured with mesenchymal stem cells via the MAPK-dependent pathway. Stem Cell Research and Therapy. 2020;11(1):537.
61. Genova T, Petrillo S, Zicola E, Roato I, Ferracini R, Tolosano E, et al. The crosstalk between osteodifferentiating stem cells and endothelial cells promotes angiogenesis and bone formation. Frontiers in Physiology. 2019;10.
62. He Y, Lin S, Ao Q, He X. The co-culture of ASCs and EPCs promotes vascularized bone regeneration in critical-sized bone defects of cranial bone in rats. Stem Cell Research and Therapy. 2020;11(1):338.
63. Fong CY, Peh GS, Gauthaman K, Bongso A. Separation of SSEA-4 and TRA-1-60 labelled undifferentiated human embryonic stem cells from a heterogeneous cell population using Magnetic-Activated Cell Sorting (MACS) and Fluorescence-Activated Cell Sorting (FACS). Stem Cell Rev Rep. 2009;5(1):72-80.
64. Lin G, Garcia M, Ning H, Banie L, Guo YL, Lue TF, et al. Defining stem and progenitor cells within adipose tissue. Stem Cells Dev. 2008;17(6):1053-63.
65. Thitilertdecha P, Lohsiriwat V, Poungpairoj P, Tantithavorn V, Onlamoon N. Extensive characterization of mesenchymal stem cell marker expression on freshly isolated and *in-vitro* expanded human adipose-derived stem cells from breast cancer patients. Stem Cells International. 2020;2020:8237197.
66. Agostini F, Rossi FM, Aldinucci D, Battiston M, Lombardi E, Zanolin S, et al. Improved GMP compliant approach to manipulate lipoaspirates, to cryopreserve stromal vascular fraction and to expand adipose stem cells in xeno-free media. Stem Cell Research and Therapy. 2018;9(1):130.
67. Asahara T, Murohara T, Sullivan A, Silver M, van der Zee R, Li T, et al. Isolation of putative progenitor endothelial cells for angiogenesis. Science. 1997;275(5302):964-7.
68. Bourin P, Bunnell BA, Casteilla L, Dominici M, Katz AJ, March KL, et al. Stromal cells from the adipose tissue-derived stromal vascular fraction and culture expanded adipose tissue-derived stromal/stem cells: A joint statement of the International Federation for Adipose Therapeutics and Science (IFATS) and the International Society for Cellular Therapy (ISCT). Cytotherapy. 2013;15(6):641-8.
69. Maumus M, Peyrafitte JA, D'Angelo R, Fournier-Wirth C, Bouloumié A, Casteilla L, et al. Native human adipose stromal cells: localization, morphology and phenotype. Int J Obes (Lond). 2011;35(9):1141-53.
70. Ho CM, Chen YH, Ho SL, Chen HY, Chien CS, Chen JC, et al. Therapeutic efficacy of adipose-derived stromal vascular fraction cells is associated with CD34 positivity in acute-on-chronic liver failure. Cytotherapy. 2019;21(5):561-5.
71. Stripecke R, Carmen Villacres M, Skelton D, Satake N, Halene S, Kohn D. Immune response to green fluorescent protein: Implications for gene therapy. Gene therapy. 1999;6(7):1305-12.
72. Quah BJC, Warren HS, Parish CR. Monitoring lymphocyte proliferation *in-vitro* and *in-vivo* with the intracellular fluorescent

dye carboxyfluorescein diacetate succinimidyl ester. Nature Protocols. 2007;2(9):2049-56.
73. Gutiérrez L, Stepien G, Gutiérrez L, Pérez-Hernández M, Pardo J, Pardo J, et al. Nanotechnology in Drug Discovery and Development. In: Chackalamannil S, Rotella D, Ward SE, editors. Comprehensive Medicinal Chemistry III. Oxford: Elsevier; 2017. p. 264-95.
74. Ren Q, Jiang C, Liu J. CFDA-SE Combined with MACSiBeads™ Particles to Evaluate the Inhibitory Effect of Treg Cells *in-vitro*. Ann Clin Lab Sci. 2019;49(6):740-7.
75. Preda MB, Neculachi CA, Fenyo IM, Vacaru A-M, Publik MA, Simionescu M, et al. Short lifespan of syngeneic transplanted MSC is a consequence of *in-vivo* apoptosis and immune cell recruitment in mice. Cell Death and Disease. 2021;12(6):566.
76. Wilson SM, Goldwasser MS, Clark SG, Monaco E, Rodriguez-Zas S, Hurley WL, et al. Adipose-derived stem migration in the vascular system after transplantation and the potential colonization of ectopic sites in Swine. J Reg Med Biol Res. 2021;2(3):1-26.

Supplementary File 1

Nodule measurement by Image J

1. Minimum of 4 pictures per well with 100x magnification were taken by a Nikon Diaphot Inverted Tissue Culture Microscope using a Nikon Digital Eclipse DXM 1200 high-resolution color digital camera and saves as JPEG file
2. Image J was scaled using a hematocytometer with the same magnification as the pictures
3. Pictures were then uploaded into ImageJ and transformed in 8 bit images by Image/Type/8-bit
4. A threshold was automatic selected by Image/Adjust/Threshold and "Apply" was selected
5. The transformed picture was used for automatic measurement of number and area of the nodules using the Analyze/Analyze Particles feature by setting the minimum area deemed to be a nodule. The diameter was then obtained by inference from the area